

# CLOSE FORMATION FLIGHT OF PASSIVE RECEIVING MICRO-SATELLITES

Hauke Fiedler<sup>(1)</sup> and Gerhard Krieger<sup>(2)</sup>

<sup>(1)</sup>*DLR, HR, Weßling, Germany, E-mail:hauke.fiedler@dlr.de*

<sup>(2)</sup>*DLR, HR, Weßling, Germany, E-mail:gerhard.krieger@dlr.de*

## ABSTRACT

Synthetic aperture radar interferometry is a powerful technique for deriving highly accurate digital elevation models on a global scale. To keep costs low, receive only satellites have been proposed to fly in close formation with an illuminating radar satellite. A new formation, called Trinodal Pendulum, is introduced and described in detail. Results of a performance estimation, flight dynamics analysis, and safety investigation are presented adopting this formation to the planned TerraSAR-L satellite. It is shown, that a global Digital Elevation Model (DEM) according to the High Resolution Terrain Information (HRTI) level 3 standard can be derived within less than 1½ years.

## 1. INTRODUCTION

One major topic in remote sensing is the derivation of a highly accurate digital elevation model (DEM) on a global scale [1]. A powerful technique to derive such a DEM is synthetic aperture radar (SAR) interferometry, which combines different SAR images of the same scene acquired from slightly different angles of incidence [1-4]. However, the accuracy of current spaceborne SAR interferometers is limited by either temporal de-correlation (repeat pass interferometry) [4] or by the achievable length of the baseline, (Shuttle Radar Topography Mission, SRTM, with a boom length of 60m) [3,5]. Several suggestions have been made to overcome these limitations, which are all based on the use of two or more spacecraft flying in close formation [1,6-10]. One example is the Radarsat 2/3 tandem which would use two almost identical SAR satellites [7]. As an alternative, it has been suggested to enhance a conventional SAR satellite like ALOS, Envisat, or TerraSAR-L by a formation of passive SAR receivers [6,9,12]. Since only passive receivers with small antennas and low power demands are required in this concept, it will allow for a cost efficient implementation by using small and cheap micro-satellites. The requirements to such a formation are manifold: The single micro-satellites should monitor the same scene only with slightly different angles of incidence and a very small time difference between the image acquisition (better would be: simultaneously). Since this will require a very close formation, collision avoidance becomes an important factor. One parameter, which determines the height accuracy of an interferometric image, is the so-called effective baseline. This effective

baseline is defined as the projection of the distance of the two receiving satellites onto the line of sight of one receiving satellite. There are two major aspects concerning this effective baseline: a larger effective baseline will result in a better height accuracy of the desired scene. This is due to the fact that the interferometric phase resolution, which is derived from the phase difference between the two SAR images, will increase with increasing baseline length. On the other hand, problems will arise as soon as the phase difference between close image pixels becomes as large as  $\pi$ , since it is then possible to assign different heights to a given phase value. These ambiguous heights are separated by the so-called height of ambiguity which decreases with increasing baseline length. As a consequence, small baselines will be required for an unambiguous retrieval of the height information in scenes with steep terrain gradients.

The contradicting requirements of having a large baseline for good height accuracy and a small baseline for successful phase unwrapping can be resolved by using a satellite constellation, which allows for the simultaneous interferometric data acquisition with large and small baselines at a fixed baseline ratio. One such formation is the Trinodal Pendulum, which will be presented in the next Section. In the following Sections, the performance is derived and a scenario generating a global DEM is presented, followed by conclusions in the last Section.

## 2. TRINODAL PENDULUM

The Trinodal Pendulum consists in its original configuration of three micro-satellites, orbiting with the same inclination, eccentricity, argument of perigee and semi-major axis as the illumination master satellite [11,12]. The right ascensions of the ascending node of each of the three micro-satellites are chosen in such a way that the horizontal cross-track displacements correspond to the desired effective baselines for interferometric data acquisition. Additionally, the along-track displacements between the single micro-satellites are chosen such that the micro-satellites monitor the requested scene on the Earth's surface with minimum relative time lags under the constraint that small along-track displacements will be required to avoid a collision within the formation at the northern and southern turns. The Trinodal Pendulum is a very stable flight formation

as all satellites will be exposed to almost the same drag, geoid potential and solar/moon/planetary forces. However, due to differences in their respective ballistic coefficients, it is possible that the micro-satellites change their along-track displacements, which must be taken into account by some form of autonomous control. An alternative is a slight modification of the orbit formation such that the orbits have an additional vertical separation at the northern and southern turns [13]. This can be achieved by a relative shift of the eccentricity vectors of the micro-satellites. One of the three micro-satellites can be kept at the master's eccentricity while the two other micro-satellites will be adopted in their eccentricities such that their relative motion follows an ellipse in the along-track/radial plane with the desired vertical separation. The radial separation between the two micro-satellites can be chosen rather small (e.g.  $\sim 500$  m), since a high momentum would be required to compensate this radial shift within a reasonable time span. Moreover, any velocity change would result in a significant increase of the along-track displacements between the satellites, which further increases the safety of the constellation. An artist's view of such a formation is given in Fig. 1.

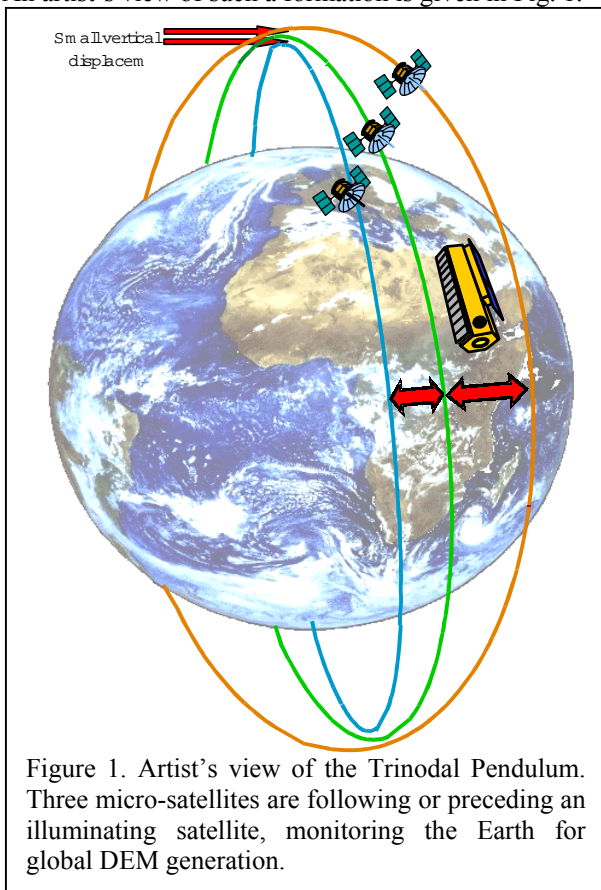


Figure 1. Artist's view of the Trinodal Pendulum. Three micro-satellites are following or preceding an illuminating satellite, monitoring the Earth for global DEM generation.

The small arrows at the northern turn mark the vertical displacements arising from the shifts of the eccentricity vectors. The large bidirectional arrows mark the horizontal baselines between the three satellites, which are necessary for the interferometric products. It is clear that the horizontal baselines decrease at higher latitudes.

This can be compensated by separation maneuvers which change the right ascensions of the ascending nodes to the desired values.

As shown in Fig. 2, two of the micro-satellites are orbiting on a relative ellipse with an aspect ratio of 1:2. These two ellipses can now be shifted in along-track, which enables an arbitrary adjustment of along-track baselines for any requested latitude without increasing

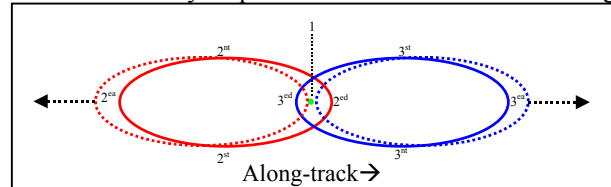


Figure 2. Relative movement of the three micro-satellites (solid lines) projected onto the orbital plane of TerraSAR-L. Satellite 1 (centred) is at a fixed position in the centre of the relative frame, while satellite 2 (left ellipses) and satellite 3 (right ellipses) form two equal ellipses which can be shifted arbitrarily in along-track. The positions of the micro-satellites are shown for the southern turn (st), for the equator in an ascending orbit (ea), for the northern turn (nt) and for the equator in the descending orbit (ed). The position between the two ellipses may be shifted arbitrarily in along-track, resulting in a zero along-track displacement at any selectable latitude (dotted lines).

the collision risk. This can for example be used for ocean calibration, where the along-track displacement between interferometric images should be as small as possible.

Now we are able to build up a formation based on the assumptions given above. We apply the parameters given in Table 1 and Table 2 for the satellites. For the flight dynamic point of view, we apply as a worst case assumption an F10.7cm flux value of  $250 \cdot 10^{-22}$  Ws/m<sup>2</sup> to the data representing solar maximum, for solar minimum we apply an F10.7cm flux value of  $75 \cdot 10^{-22}$  Ws/m<sup>2</sup>. For modelling the Earth, we include an Earth gravity field with coefficients up to degree and order 70. The simulation includes furthermore sun and moon perturbations as well as solar radiation pressure.

Table 1. Parameters of TerraSAR-L as illuminating satellite.

TerraSAR-L Parameters	Value
Eccentricity	0.00114
Semi-major axis	7007.137km
Inclination	97.93°
Argument of perigee	90°
Mass	2600kg
Cross section	3m <sup>2</sup>
Right ascension of the ascending node	0°
True anomaly	270°

Table 2. Parameters of the micro-satellites forming a relative ellipse with 500m radial diameter.

Micro-SAT Parameters	Satellite 1	Satellite 2	Satellite 3
Eccentricity	0.00114	0.001073	0.001216
Semi-major axis	7007.137km	7007.137km	7007.137km
Inclination	97.93°	97.93°	97.93°
Argument of perigee	90°	90°	90°
Mass	130kg	130kg	130kg
Cross section	1m <sup>2</sup>	1m <sup>2</sup>	1m <sup>2</sup>
Right asc. of asc. Node	0°	0.01171°	0.09325°
True anomaly	269.99677°	270.00622°	269.99705°

In the originally proposed formation of the Trinodal Pendulum, the eccentricity values would be the same as the ones of TerraSAR-L. In the safer mode, as described above, the eccentricities for the three micro-satellites are not equal, resulting in a rotation of their respective eccentricity vectors with a period of ~111days due to secular disturbances. This might be stabilised by keeping the argument of perigee within a certain range. For example, a phase of 30° corresponding to 9.25days would keep the vertical displacement in a range of ±1.7% or ±5m for the ellipse. This, of course, will require additional fuel and manoeuvring. For the values mentioned above, the additional fuel will be in the order of 0.305kg/year, which is affordable. Also a cycle time of ~9.3days is reasonable.

The next point of this formation is the stability of the interferometric baselines, since the small differences in

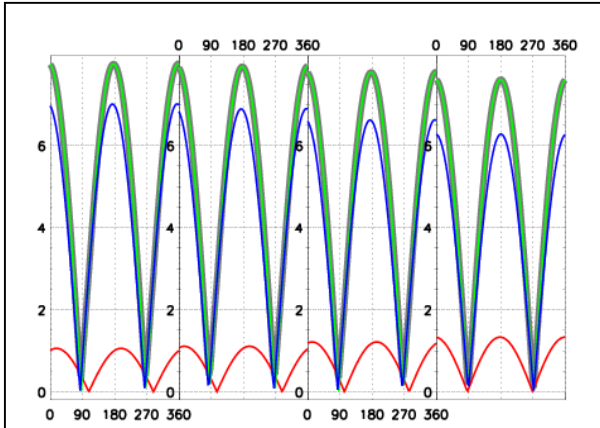


Figure 3. Effective baselines in [km] vs. argument of latitude. The effective baselines are very stable. We show the long time evolution of a whole orbit in the beginning, after 3 days, after 10 days and after 30 days. The different colors mark the different baselines between the micro-satellites. The stability is almost independent of solar flux activity. The small variations of the effective baselines are due to the difference in the respective eccentricity vectors.

the satellites eccentricity vector will result in a motion of libration, which will vary the maximum value of the effective baselines. This effect is very small as demonstrated in Fig. 3. Furthermore, the motion of the libration of the long periodic argument of perigee can be seen in the same plot, in which the maximum effective baselines are oscillating slightly forth and back around 90°.

The effective baselines in the Trinodal Pendulum will become smaller for higher latitudes. If a decrease of an initially chosen interferometric baseline is tolerated up to 50%, the Earth's surface between -60° and +60° of latitude can be mapped without any formation change. Note that this area makes already ~80% of the global land area. Higher latitudes will require a change of the formation. This may be achieved by a change of the initially selected right ascensions of the ascending nodes, which will allow larger effective baselines with the same stability of the formation. For pole mapping and/or very high latitudes another formation has to be selected. Section IV will present an appropriate acquisition strategy for the generation of a global DEM.

### 3. PERFORMANCE ANALYSIS

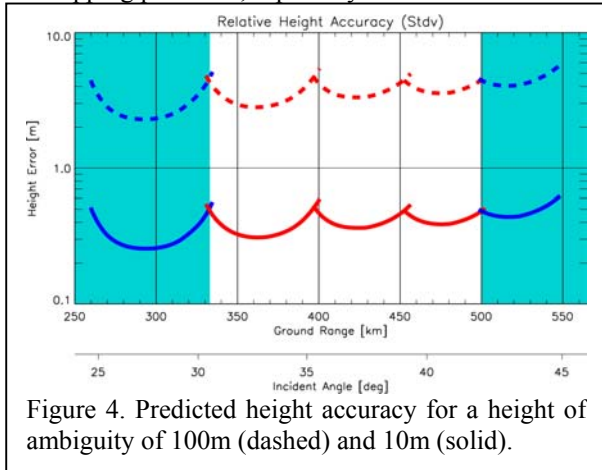
In the following, we will summarize some results from a derivation of the achievable height accuracy (details of the performance analysis may be found in [9] and [12]). For illustration purposes, we assume here the acquisition of a 168 km swath using three sub-swaths. The value of 168 km corresponds to the separation of the satellite ground tracks at the equator after one full repeat cycle of 16 days of TerraSAR-L. Table 3 summarizes the main parameters of a possible sub-swath partitioning. The sub-swath selection results from a first, rough iteration, which had the goal to optimize the DEM performance across a swath of 168 km with a minimum number of sub-swaths.

Table 3. Summary of System, Processing, and Beam Parameters.

Swath selection option			
Swath Width	70 km	60 km	50 km
Antenna Look Angle	29.2	33.7	36.6
Incident Angles [deg]	30.3 – 35.5	35.2 – 39.3	39.0 – 42.2
PRF [Hz]	2190	2490	2200
Ground Range [km]	330 – 400	396 – 456	452 – 502
Antenna Tapering	Taylor	None	Taylor
Processed Bandwidth [Hz]	1200	1000	1200

Figure 4 shows the predicted height accuracy for a height of ambiguity of 100m (dashed) and 10m (solid). It is obvious, that the height accuracy increases with a decreasing height of ambiguity. On the other hand, a

small height of ambiguity is likely to cause phase unwrapping problems, especially in mountainous areas.



Note that the baseline ratio of the example in Figure 4 has been chosen such that the height errors from the DEM acquisition with the small baseline stay below the height of ambiguity for the large baseline. It would hence be possible to use the interferometric data from the small baseline to assist phase unwrapping in the highly sensitive large baseline interferogram.

#### 4. DEM GENERATION SCENARIO

This section introduces a possible scenario for the acquisition of a global DEM. For this, we assume that the mean monitoring time of the three micro-satellites is 180s per orbit. The global land area is assumed to be  $149 \cdot 10^6 \text{ km}^2$ . We furthermore assume that each area must be mapped twice, once with an ascending and once with a descending orbit, to acquire a DEM with high quality.

Now, with all the assumptions above, we are able to construct a scenario for deriving a global DEM based on the Trinodal Pendulum, orbiting in front of TerraSAR-L. For this, we divide the Earth in sections depending on latitude as shown in Table 4. Each section will be mapped with an individual number of sub-swaths depending on the swath width. Furthermore, we give also in the same Table the mapped land area in  $\text{km}^2$  and in percent. It is obvious that with increasing latitude the ground swath will decrease. This results in a smaller number of required sub-swaths. Furthermore, higher latitudes than  $75^\circ$  can not be mapped with the Trinodal Pendulum formation as the horizontal baselines will become too small. Therefore, a change of the formation in the last stage of the scenario is necessary which will be explained below.

First, the Trinodal Pendulum is set up as described above with resulting horizontal baselines of 8km, 6.4km, and 1.6km at the equator. This will enable to monitor the Earth between latitudes  $\pm 30^\circ$ . When completing this first part, the right ascensions of the ascending nodes are widened up resulting in a horizontal separation of 9km, 7.2km, and 1.8km. This will enable mapping the second part of the Earth,

between latitudes of  $30^\circ$  and  $50^\circ$  on the northern and southern hemisphere. This procedure is repeated twice, with separations of the right ascensions of the ascending nodes of 12km, 9.6km, and 2.4km at first followed by separations of 18km, 14.4km, and 3.6km. For the last part, mapping the Earth at highest latitudes ( $> \pm 75^\circ$ ), the formation will be changed. The inclination of all satellites will be changed in such a way that the resulting drift in the right ascension of the ascending node of each individual micro-satellite will result in a right ascension of the ascending node of  $0^\circ$  after 45days. Due to the new inclinations, the three micro-satellites will span new effective baselines at high latitudes, capable of mapping the remaining 5.7% of the Earth's surface. The theoretical minimum time span for mapping such an area is less than 16days. Therefore, 45days as assumed above should suffice for mapping this area including at least one ascending and one descending orbit. Also, the swath overlap should be enough for this scenario. The complete scenario is summarized in Table 5. In the same table the estimates of fuel consumption for formation changing are also given.

#### 5. DISCUSSION

SAR interferometry is a powerful technique for the derivation of digital elevation models on a global scale. For optimum performance, this technique will require satellite formations with well defined interferometric baselines. The required baselines can be provided by either a radial or a cross track displacement between the monitoring satellites. Furthermore, the interferometric data should be recorded with relative time differences which are as short as possible to minimize decorrelation effects. Hence, very close and stable satellite formations will be required. Unfortunately, some of the Keplerian parameters of a satellite result in drifts: a difference in inclination will result in an unintentional drift of the right ascension of the ascending node, a difference in eccentricity will result in a drift in along-track – both due to geoid, the latter additionally due to differential drag. But, as different look angles are required, the monitoring satellites cannot orbit behind each another. Therefore, the simplest formation will be a configuration in which all satellites have the same eccentricity and inclination, but differ in the right ascension of the ascending nodes for setting up the requested look angle difference. In case of three satellites, this formation is denoted as the Trinodal Pendulum. Note that there is always a small risk of collision at the northern and southern turn, where the satellites differ in along-track only. Collision avoidance would be possible by a slight shift in their true anomalies. However, an along track displacement between the single satellites might not be enough if short along-track displacements are required. With e.g. different ballistic coefficients, the single satellites will be exposed to different frictions by drag, which will

Table 5. Detailed mission scenario based on the Trinodal Pendulum.

Time [days]	Description of Mission	Fuel [kg] S1/S2/S3	DEM [%] (passes)
-x till 0	Formation set-up of the Trinodal Pendulum, testing and calibrations. The distance at the equator between the right ascensions of the ascending node will be [8km,6.4km,1.6km], symmetrically distributed around the right ascension of the ascending node of the master satellite.	S1: 0.200 S2: 0.120 S3: 0.200	0
0-99	Mapping the first latitude range between 0° and 30°. Here, we assume four beams. For convenience we assume all orbits to be ascending ones. The total area of $67.1 \cdot 10^6 \text{km}^2$ is mapped with two effective baselines simultaneously.		45.1(1)
100-199	The same area is mapped with descending orbits.		45.1(2)
200-206	Now the Trinodal Pendulum will be separated in the right ascension of the ascending node by [1km,2km,4km] resulting in distances in the right ascension of the ascending nodes at the equator of [9km,7.2km,1.8km]. The maneuver should be executed and fine-tuned within 7 days.	S1: 0.025 S2: 0.015 S3: 0.025	45.1(2)
207-256	With the new baselines the latitudes of $\pm[30^\circ,50^\circ]$ are mapped with three beams, including an area of $37.2 \cdot 10^6 \text{km}^2$ , resulting in $\sim 25.0\%$ of the total area.		45.1(2) +25.0(1)
257-306	The same is done with the missing ascending or descending orbits, resulting in the same time.		70.1(2)
307-311	Again, the Trinodal Pendulum is widened in its right ascensions of the ascending nodes to [12km,9.6km,2.4km]. The maneuver is executed and calibrated within 5days due to the experience gained within the days 200-206.	S1: 0.075 S2: 0.045 S3: 0.075	70.1(2)
312-342	With the new baselines the latitudes of $\pm[50^\circ,65^\circ]$ are mapped with two beams, including an area of $22.1 \cdot 10^6 \text{km}^2$ , resulting in $\sim 14.8\%$ of the total area. Again, all orbits are assumed to be descending ones.		70.1(2) +14.8(1)
343-373	The same area is mapped with ascending orbits. The same time will be required.		84.9(2)
374-377	One more time the Trinodal Pendulum is widened in its distances at the equator to [18km,14.4km,3.6km]. The expected time for maneuvering and calibration is believed to be 5days.	S1: 0.150 S2: 0.090 S3: 0.150	84.9(2)
378-395	With the new baselines the latitudes of $\pm[65^\circ,75^\circ]$ are mapped with a single beam, including an area of $14.0 \cdot 10^6 \text{km}^2$ , resulting in $\sim 9.4\%$ of the total area. All orbits are assumed to be descending ones.		84.9(2) +9.4(1)
396-413	The same region is mapped with ascending orbits. The same time will be required.		94.3(2)
414-458	Now the formation is changed. The inclination will be changed for the two micro-satellites S1 and S3 in such a manner that the drift per day in the right ascension of the ascending nodes will be 200m per day relative to the master satellite. For the micro-satellite S2 the drift should be 120m per day. The direction of the drift will be selected in such a manner that the right ascension of the ascending nodes will be 0° after 45days. The shift in inclination will be $\sim 0.01^\circ$ for S1 and S3, and $\sim 0.006^\circ$ for S2. During this time, due to the different inclinations, the micro-satellites will span new effective baselines capable of mapping latitudes between $\pm[75^\circ,90^\circ]$ . The land area is $8.6 \cdot 10^6 \text{km}^2$ , resulting in $\sim 5.7\%$ of the total area. By skillfully selecting the swathes with a maximum overlap of 50%, the leaving area can be mapped with one pass in $\sim 16$ days. Thus, the 45days as described above are a worst case assumption leaving enough margins for mapping the left area with at least a second pass.	S1: 0.060 S2: 0.040 S3: 0.060	100(2)
459-463	Now all satellites will be shifted back in inclination, requiring the same amount of fuel. This manoeuvre will last 5 days.	S1: 0.060 S2: 0.040 S3: 0.060	100(2)
463	As a break, we will estimate the total fuel consumption for each micro-satellite without orbit keeping manoeuvres applied.	S1: 0.570 S2: 0.350 S3: 0.570	100(2)
464-548	For the rest of the 1.5years mission time, secondary mission goals may be applied as well as different formations for 85days. Furthermore, specific regions may be mapped if requested without any problem due to the few fuel consumption of the mission.		100

result in a drift in along-track. This can easily happen if e.g. the cross sections differ or if the fuel consumption of the satellites is not the same. This collision risk can be avoided by an additional eccentricity separation [14,15]. The small difference in the eccentricity vectors of the single satellites results in a motion in radial and along track direction. In the beginning of this motion of libration, the maximum radial separation will occur at the northern and southern turns, which will minimize the risk of a collision. Note, that the orbits are now completely separated, which allows in principle an arbitrary shift of the satellites along their orbits. For maximizing collision avoidance, the respective arguments of perigee might be kept in an interval in such a way that the single satellites do not complete a full motion of libration. Here, the satellites do not describe a full ellipse in the relative frame of motion. This implies, that additional maneuvering and fuel is requested in order to keep the arguments of perigee in a certain interval of e.g.  $\pm 30^\circ$  in phase. These additional maneuvers might be combined with the formation and/or station keeping maneuvers to minimize fuel consumption. Now, with such a formation, we end up with stable effective baselines, in which the single satellites can monitor the desired acquisition area with very short time differences.

Based upon this formation, we have estimated the interferometric SAR performance taking into account different error sources like SNR decorrelation, ambiguities in range and azimuth, data quantization, etc. Adopting the radar and satellite parameters of TerraSAR-L, the Trinodal Pendulum will enable the acquisition of a global DEM according to NIMA HRTI-3 standard in less than 1½ years.

## 6. ACKNOWLEDGEMENT

We would like to thank M. Zink, R. Torres, B. Duesmann, and G. Levrini from ESA for initiation and support of this work. The numerous and fruitful discussions with M. Werner, F. Douchin, F. Jochim, T. Amiot, A. Moreira, J. Fourcade, J.C. Souyris, C. Jouve, H. Runge, F. Rocca, R. Romeiser, K. Papathanassiou, and I. Hajnsek during the joint ESA-DLR-CNES meetings are greatly appreciated. Financial support for this work came from ESA.

## 7. REFERENCES

1. Zebker, H., Farr, T., Salazar, R., and Dixon, T., "Mapping the World's Topography Using Radar Interferometry: The TOPSAT Mission," Proceedings of the IEEE, Vol. 82, No. 12, 1994, pp. 1774-1786.
2. Bamler, R. and P. Hartl, "Synthetic Aperture Radar Interferometry," Inverse Problems, Vol. 14, 1998, pp. R1-R54
3. Rosen, P.A., Hensley, S., Joughin, I.R., Li, F.K., Madsen, S.N., Rodriguez, E., Goldstein, R., "Synthetic

- Aperture Radar Interferometry," Proceedings of the IEEE, Vol. 88, No. 3, 2000, pp. 333-382.
4. Hanssen, R.F., Radar Interferometry, Kluwer Academic Publishers, Dordrecht, 2001.
5. Werner, M. "Shuttle Radar Topography Mission (SRTM): Mission Overview," Journal of Telecommunication (Frequenz), Vol. 55, No. 3-4, 2001, pp. 75-79.
6. Massonnet D., "Capabilities and Limitations of the Interferometric Cartwheel," IEEE Trans. Geosci. Remote Sensing, Vol. 39, No. 3, 2001, pp. 506-520.
7. Evans N.B., Lee P., and Girard R., "The Radarsat 2&3 Topographic Mission: An Overview," Proceedings IGARSS'02 (CD-Rom), Toronto, Canada, 22-26 June 2002.
8. Martin M., Klupar P., Kilberg S., Winter J., "TechSat 21 and Revolutionizing Space Missions Using Microsatellites," American Institute of Aeronautics and Astronautics, 2001.
9. Krieger G., Fiedler H., Mittermayer J., Papathanassiou K., and Moreira A., "Analysis of Multistatic Configurations for Spaceborne SAR Interferometry," IEE Proceedings – Radar, Sonar, Navigation, Vol. 150, No. 3, pp. 87-96, 2003.
10. Moreira, A. et al., "TanDEM-X: A TerraSAR-X Add-On Satellite for Single-Pass SAR Interferometry," IGARSS 2004, Anchorage, USA.
11. Fiedler, H., Krieger, G., "Formation Flying Concepts", Intermediate Presentation to ESA TS-SW-ESA-SY-0002, Toulouse, June 2003.
12. Zink, M., Krieger, G., Amiot, T., "Interferometric Performance of a Cartwheel Constellation for TerraSAR-L," Fringe Workshop, Frascati, Italy, 2003.
13. Fiedler, H., Krieger, G., Jochim, F., "Analysis of TerraSAR-L Cartwheel constellations - Amendment", Technical Note, DLR, Oberpfaffenhofen, November 2003.
14. Wauthier, P., Bischops, E., Francken, Ph., Hooge, M., Laroche, H., "On the co-location of eight Astra satellites", International Symposium on Space Flight Dynamics, Biarritz, 2000
15. Kirschner M., Montenbruck O., D'Amico S., "Safe Switching of the GRACE Formation using an Eccentricity/Inclination Vector Separation", to be presented at 18th International Symposium on Space Flight Dynamics, 11-15 Oct. 2004, Munich, Germany